seen because of their very broad widths and low elasticities. Several of the resonances on the other trajectories might be seen, however. The resonances of the Δ_δ' trajectory have relatively high elasticities in our model, a property that favors observation, but they have large widths, a property which makes observation difficult. The situation is the opposite for the resonances of the Δ_γ trajectory, which have relatively small widths (favoring observation) and small elasticities (making observation difficult).

It is interesting, however, that the use of the set of resonances proposed in this paper gives[19] a fair agreement to the observed π^+p total cross section once the diffraction contribution has been subtracted out.

An important test of the model would be a comparison with polarization data. Unfortunately, only preliminary π^+p backward polarization data exist.[20] Therefore, without attempting to make a fit to these preliminary data, we simply predict the polarization for an incident momentum of 2.75 GeV/c. This is shown in Fig. 8. The remarkable feature of this prediction is that it qualitatively agrees with the preliminary data of Ref. 18 in that it is positive in the backward direction and changes sign near the position of the dip in the angular distribution. Since the polarization depends very sensitively on the exact values of the parameters, we expect that a slight change in the parameters could lead to a more quantitative agreement with the final data.

Lacking more complete experimental data on higher recurrences of the Regge trajectories, one might consider comparing our elasticities (Fig. 3) with those predicted by the Veneziano model.[21] At the moment the conclusion seems to be that the Veneziano model "...fails to provide an adequate extrapolation from the scattering data to the widths of the Δ_δ (1238) and its recurrences."[22]

We do not wish to claim that all the trajectories of our model really exist. Our main point is that by including resonances lying on trajectories other than the Δ_δ, we can obtain the qualitative characteristic behavior of the observed π^+p cross section in an angular range near the backward direction. We therefore take it as quite plausible that at least one additional Δ trajectory exists. Such a trajectory is necessary if duality is meaningful at these energies.

Because of the reasonable success of the model, we are at present extending the calculations to include the angular distributions and polarization at all angles, adding the forward diffraction peak as a separate contribution.

ACKNOWLEDGMENTS

We appreciate the contributions of J. P. Chandler and R. A. Sidwell to this work.

[19] M. Ciftan and G. Patsakos (private communication).
[20] N. Booth, G. Conforto, and A. Yokosawa, presented by G. Bellettini, in *Proceedings of the Fourteenth International Conference on High-Energy Physics, Vienna, 1968* (CERN, Geneva, 1968), p. 329.
[21] G. Veneziano, Nnovo Cimento **57A**, 190 (1968).
[22] E. L. Berger and G. C. Fox, Phys. Rev. **188**, 2120 (1969).

PHYSICAL REVIEW D VOLUME 1, NUMBER 1 1 JANUARY 1970

Electroproduction of Nucleon Resonances and Implications for Coincidence Experiments*

P. L. PRITCHETT† AND P. A. ZUCKER†
Institute of Theoretical Physics, Department of Physics, Stanford University, Stanford, California 94305
(Received 14 July 1969)

The general form of the coincidence cross section for electroproduction of nucleon resonances is reviewed and discussed using the helicity formalism. The predictions of a coupled-channel relativistic N/D model are discussed for nucleon levels in the first four resonance regions. These predictions serve to indicate important questions concerning the structure of the nucleon, and consideration is given as to how these questions may be answered by means of coincidence experiments.

I. INTRODUCTION

ELECTRON excitation has now become a practical means for studying the detailed structure of the excited states of the nucleon. In most experiments performed so far, only the final electron has been detected. Some experiments detecting the final charged pion or nucleon in coincidence with the electron have been performed in the $N^*(1236)$ region,[1–5] and extensive coincidence experiments are planned for the higher

* Research sponsored by the Air Force Office of Scientific Research, Office of Aerospace Research, U. S. Air Force, under AFOSR Contract No. F44620-68-C-0075.
† National Science Foundation Predoctoral Fellow.
[1] W. W. Ash, K. Berkelman, C. A. Lichtenstein, A. Ramanauskas, and R. H. Siemann, Phys. Letters **24B**, 165 (1967).
[2] C. W. Akerlof, W. W. Ash, K. Berkelman, C. A. Lichtenstein, A. Ramanauskas, and R. H. Siemann, Phys. Rev. **163**, 1482 (1967).
[3] C. Mistretta, D. Imrie, J. A. Appel, R. Budnitz, L. Carroll, J. Chen, J. Dunning, Jr., M. Goitein, K. Hanson, A. Litke, and R. Wilson, Phys. Rev. Letters **20**, 1070 (1968); D. Imrie, C. Mistretta, and Richard Wilson, *ibid.* **20**, 1074 (1968).
[4] C. Mistretta, D. Imrie, J. A. Appel, R. Budnitz, L. Carrol, M. Goitein, K. Hanson, and Richard Wilson, Phys. Rev. Letters **20**, 1523 (1968).
[5] K. Baba, N. Kajiura, S. Kanejo, K. Huke, R. Kikuchi, Y. Kobayashi, and T. Yamakawa, Nuovo Cimento **59A**, 53 (1969).

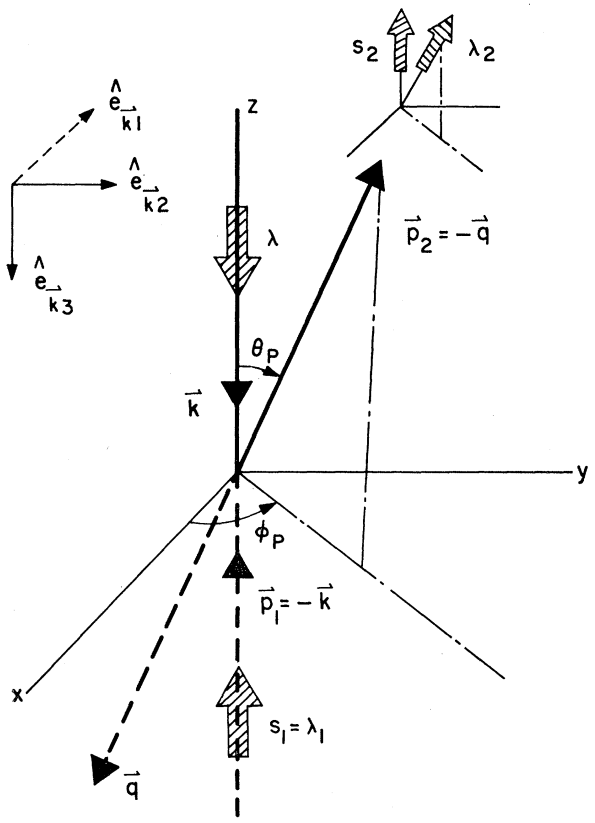

FIG. 1. Choice of angles and helicity unit vectors in the center-of-momentum frame.

resonance region.[6] It is therefore important to examine what can be learned from coincidence measurements in general and to discuss how particular theoretical predictions can be most easily tested using coincidence techniques. This is of interest both in planning and interpreting experiments as well as in testing our present understanding of the nucleon resonances.

In Sec. II we review what can be said about coincidence experiments on general grounds. An expression for the coincidence cross section is given in terms of matrix elements of the nucleon current. The dependence of these matrix elements on the c.m. angles is displayed through a Jacob-Wick helicity analysis. The angular dependence associated with resonances of low spin is noted in particular, while the general partial-wave expansion is summarized in Appendix B. Measurement of this angular dependence permits a direct determination of the spin of a resonance as well as a separation of the form factors describing the excitation of the resonance. The particular advantages of making measurements in the forward (or backward) direction in the c.m. system are also discussed.

To go beyond the general discussion of Sec. II and make specific predictions for the excitation of nucleon resonances, it is necessary to use a model. In Sec. III we present predictions for the individual form factors based on a coupled-channel relativistic N/D model. The results of this model have been compared previously with the noncoincidence data,[7,8] and the agreement is good. It has been found, however, that widely differing models can all give reasonable fits to the noncoincidence cross section despite making quite different predictions for the individual form factors.[9] Since coincidence experiments permit the determination of these form factors, such experiments will provide a much more stringent test of our present understanding of the resonances. In Sec. IV we discuss some distinctive predictions of the relativistic N/D model and indicate how they can be tested in coincidence experiments. Section V contains a brief summary.

Appendix A summarizes the notation and conventions and compares them to others frequently used. Some suggestions for separating the resonant part of a measured amplitude are also presented.

II. GENERAL DISCUSSION OF COINCIDENCE EXPERIMENTS

The general form of the coincidence cross section has been discussed by several authors.[7,10–15] We will use the notation and results of Pritchett, Walecka, and Zucker.[7] We shall consider the $|\pi N\rangle$ final state explicitly, but the general discussion is directly applicable to other two-body final states such as $|\pi N^*(1236)\rangle$.

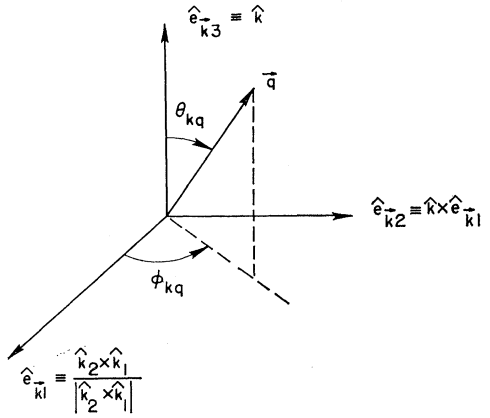

FIG. 2. Relation of the transverse unit vectors to the initial and final electron momenta. The pion angles θ_{kq} and ϕ_{kq} are also indicated.

[6] F. Pipkin (private communication).

[7] P. L. Pritchett, J. D. Walecka, and P. A. Zucker, Phys. Rev. **184**, 1825 (1969).

[8] J. D. Walecka and P. A. Zucker, Phys. Rev. **167**, 1479 (1968).

[9] P. L. Pritchett, N. S. Thornber, J. D. Walecka, and P. A. Zucker, Phys. Letters **27B**, 168 (1968).

[10] H. F. Jones, Nuovo Cimento **40A**, 1018 (1965).

[11] P. Kessler, Ann. Inst. Henri Poincaré (A)**3**, 363 (1965).

[12] K. Berkelman, in *Proceedings of the International Symposium on Electron and Photon Interaction at High Energies, Hamburg, 1965* (Deutsche Physikalishe Gesellschaft e.V., Hamburg, Germany, 1966), Vol. II, p. 299.

[13] N. Christ and T. D. Lee, Phys. Rev. **143**, 1310 (1966).

[14] N. Zagury, Nuovo Cimento **52A**, 506 (1967); **54A**, 211(E) (1968).

[15] Stephen L. Adler, Ann. Phys. (N. Y.) **50**, 189 (1968).

Following Walecka and Zucker,[8] we choose a coordinate system in the c.m. frame of the pion and final nucleon as indicated in Fig. 1. The matrix elements of the nucleon current are denoted by[16]

$$\mathfrak{J}_\mu \equiv (m/4\pi W)(2\omega_q E_1 E_2 \Omega^3/m^2)^{1/2} \times \langle p_2 q^{(-)} | J_\mu(0) | p_1 \rangle, \quad (2.1)$$

$$J_\mu(0) \equiv (\mathbf{J}(0), iJ_c(0)). \quad (2.2)$$

Here m is the nucleon mass, while W is the total energy and E_1, E_2, ω_q are the nucleon and pion energies in the c.m. frame. In Fig. 2 we make a specific choice for the transverse unit vectors $\hat{e}_{k1}$ and $\hat{e}_{k2}$ in terms of the initial and final electron momenta $\mathbf{k}_1$ and $\mathbf{k}_2$. From these unit vectors we choose a spherical basis as follows:

$$\begin{aligned} \hat{e}_{\pm 1} &\equiv \mp \tfrac{1}{2}\sqrt{2}(\hat{e}_{k1} \pm i\hat{e}_{k2}), \\ \hat{e}_0 &\equiv \hat{e}_{k3}. \end{aligned} \quad (2.3)$$

We then define

$$\mathcal{J}^{\lambda_k} \equiv \mathfrak{J} \cdot \hat{e}_{\lambda_k}, \quad \lambda_k = \pm 1, 0. \quad (2.4)$$

Thus $\mathcal{J}^{\lambda_k}$ is the current matrix element for a virtual photon of helicity λ_k. From current conservation it follows that

$$\mathcal{J}_c = (k^*/k_0)\mathcal{J}^0, \quad (2.5)$$

where k^* is the magnitude of the virtual photon three-momentum in the c.m. frame, and k_0 is the energy of the virtual photon in this frame.

The general coincidence cross section is then [see Eq. (C26) of Ref. 7]

$$\frac{d^5\sigma_L}{d\epsilon_2 d\Omega_2 d\Omega_q^*/4\pi} = \frac{\alpha^2 \cos^2\frac{1}{2}\theta}{4\epsilon_1^2 \sin^4\frac{1}{2}\theta} \frac{4mq}{W} \Bigg\{ \frac{k^4}{k^{*4}} |\mathcal{J}_c|^2 + \left(\frac{k^2}{2k^{*2}} + \frac{W^2}{m^2}\tan^2\tfrac{1}{2}\theta\right)(|\mathcal{J}^{+1}|^2 + |\mathcal{J}^{-1}|^2) + \frac{k^2}{2k^{*2}} 2\,\mathrm{Re}(\mathcal{J}^{+1})^*(\mathcal{J}^{-1}) + \frac{k^2}{k^{*2}}\left(\frac{W^2}{m^2}\tan^2\tfrac{1}{2}\theta + \frac{k^2}{k^{*2}}\right)^{1/2} \times \sqrt{2}\,\mathrm{Im}\mathcal{J}_c^*(\mathcal{J}^{+1} + \mathcal{J}^{-1}) \Bigg\}, \quad (2.6)$$

where ϵ_1 is the initial electron energy and θ is the electron scattering angle, both measured in the laboratory. k^2 is the square of the four-momentum transferred to the target, q is the magnitude of the pion three-momentum in the c.m. frame, and $d\Omega_q^*$ is the solid angle in this frame.

The c.m. angular dependence of the cross section can be made explicit through an helicity analysis following Jacob and Wick[17,18]:

$$(\mathcal{J}^{\lambda_k})_{\lambda_2\lambda_1} = (4k^*q)^{-1/2} \sum_J (2J+1) \times \mathfrak{D}_{\lambda_1-\lambda_k,\lambda_2}{}^J(-\phi_p - \theta_p \phi_p)^* \times \langle \lambda_2 | T^J(W,k^2) | \lambda_1 \lambda_k \rangle, \quad (2.7)$$

$$(\mathcal{J}_c)_{\lambda_2\lambda_1} = (k^*/k_0)(4k^*q)^{-1/2} \sum_J (2J+1) \times \mathfrak{D}_{\lambda_1\lambda_2}{}^J(-\phi_p - \theta_p\phi_p)^* \times \langle \lambda_2 | T^J(W,k^2) | \lambda_1 0 \rangle. \quad (2.8)$$

By comparing Figs. 1 and 2, we see that the nucleon angles θ_p and ϕ_p are related to the pion angles θ_{kq} and ϕ_{kq} by

$$\theta_p = \theta_{kq}, \quad \phi_p = 2\pi - \phi_{kq}. \quad (2.9)$$

These expansions define the helicity matrix elements $\langle \lambda_2 | T^J(W,k^2) | \lambda_1 \lambda_k \rangle$.

It is convenient to introduce states of definite parity:

$$\begin{aligned} \langle \tfrac{1}{2}\pm | &\equiv \tfrac{1}{2}\sqrt{2}[\langle \lambda_2 = \tfrac{1}{2} | \pm \langle -\tfrac{1}{2} | \,], \\ | \tfrac{3}{2}\pm \rangle &\equiv \tfrac{1}{2}\sqrt{2}[\,| \lambda_1 = -\tfrac{1}{2}, \lambda_k = 1 \rangle \mp | \tfrac{1}{2} -1 \rangle], \\ | \tfrac{1}{2}\pm \rangle &\equiv \tfrac{1}{2}\sqrt{2}[\,| \tfrac{1}{2}\, 1 \rangle \mp | -\tfrac{1}{2}\, -1 \rangle], \\ | L^\pm \rangle &\equiv \tfrac{1}{2}\sqrt{2}[\,| \tfrac{1}{2}\, 0 \rangle \mp | -\tfrac{1}{2}\, 0 \rangle]. \end{aligned} \quad (2.10)$$

The superscript $\pm$ refers to the notation $J = l \pm \frac{1}{2}$, with l denoting the orbital angular momentum of the pion, and the parity of these states is $\pi = (-1)^{J\pm 1/2} = (-1)^{l\pm 1}$. We then introduce a shorthand notation for the matrix elements involving states of definite parity[19]:

$$\begin{aligned} T_{1/2,3/2}{}^{l\pm} &\equiv \mp \langle \tfrac{1}{2}\pm | T^J(W,k^2) | \tfrac{3}{2}\pm \rangle, \\ T_{1/2,1/2}{}^{l\pm} &\equiv \langle \tfrac{1}{2}\pm | T^J(W,k^2) | \tfrac{1}{2}\pm \rangle, \\ T_{1/2,c}{}^{l\pm} &\equiv (k^*/k_0)\langle \tfrac{1}{2}\pm | T^J(W,k^2) | L^\pm \rangle. \end{aligned} \quad (2.11)$$

When convenient, we shall use T^{J^π} as an alternative notation to $T^{l\pm}$.

If the nucleon spins are not measured, one averages over initial spins and sums over final spins. The resulting general partial-wave expansion of the cross section is given in Appendix B. If only one intermediate J^π state is important, as in the production of a resonance, the cross section has the form

$$\frac{d^5\sigma_L}{d\epsilon_2 d\Omega_2 d\Omega_q^*/4\pi} = \frac{m}{W}\sigma_M \frac{k^2}{2k^{*2}\epsilon}\frac{1}{k^*} \times \{ h_1{}^{J^\pi}(\theta_{kq})[\,|T_{1/2,1/2}{}^{J^\pi}|^2 + 2\epsilon(k^2/k^{*2})|T_{1/2,c}{}^{J^\pi}|^2] + h_3{}^{J^\pi}(\theta_{kq})|T_{1/2,3/2}{}^{J^\pi}|^2 + 2\epsilon\cos 2\phi_{kq}\, h_4{}^{J^\pi}(\theta_{kq})\,\mathrm{Re}(T_{1/2,3/2}{}^{J^\pi *}T_{1/2,1/2}{}^{J}) + 2[(k^2/k^{*2})\epsilon(\epsilon+1)]^{1/2}\sin\phi_{kq} \times h_6{}^{J^\pi}(\theta_{kq})\,\mathrm{Re}(T_{1/2,c}{}^{J^\pi *}T_{1/2,3/2}{}^{J^\pi})\}, \quad (2.12)$$

[16] We use a metric such that $a_\mu = (\mathbf{a}, ia_0)$. We set $\hbar = c = 1$, and thus $\alpha = e^2/4\pi = 1/137$.

[17] M. Jacob and G. C. Wick, Ann. Phys. (N. Y.) **7**, 404 (1959).

[18] We use the angular momentum notation of A. R. Edmonds, *Angular Momentum in Quantum Mechanics* (Princeton University Press, Princeton, N. J., 1957).

[19] We have found it convenient to work with these quantities. They are related to the "parity amplitudes" defined by Walecka and Zucker (Ref. 8) by $T_{3/2}{}^{l\pm} = \mp(4k^*q)^{-1/2}T_{1/2,3/2}{}^{l\pm}$, $T_{1/2}{}^{l\pm} = (4k^*q)^{-1/2}T_{1/2,1/2}{}^{l\pm}$, and $(k^*/k_0)L^{l\pm} = (4k^*q)^{-1/2}T_{1/2,c}{}^{l\pm}$.

TABLE I. θ_{kq} dependence of the resonance cross section [Eq. (2.12)]. (Note that $x\equiv\cos\theta_{kq}$.)

J^π	$h_1{}^{J^\pi}(\theta_{kq})$	$h_3{}^{J^\pi}(\theta_{kq})$	$h_4{}^{J^\pi}(\theta_{kq})$	$h_6{}^{J^\pi}(\theta_{kq})$
$\frac{1}{2}\pm$	1	0	0	0
$\frac{3}{2}\pm$	$1+3x^2$	$3(1-x^2)$	$-\sqrt{3}(1-x^2)$	$2\sqrt{3}x(1-x^2)^{1/2}$
$\frac{5}{2}\pm$	$(9/4)(1-2x^2+5x^4)$	$(9/8)(1-x^2)(1+15x^2)$	$-(9/8)\sqrt{2}(1-x^2)(1+5x^2)$	$-(9/4)\sqrt{2}x(1-x^2)^{1/2}(1-5x^2)$
$\frac{7}{2}\pm$	$(9/4)(1+5x^2-55x^4/3+175x^6/9)$	$(15/4)(1-x^2)$ $\times(1-6x^2+21x^4)$	$-(3/4)(\sqrt{15})(1-x^2)$ $\times(1-2x^2+35x^4/3)$	$(3/2)(\sqrt{15})x(1-x^2)^{1/2}$ $\times(1-22x^2/3+35x^4/3)$

where we have defined

$$\sigma_M\equiv\alpha^2\cos^2\tfrac{1}{2}\theta/4\epsilon_1{}^2\sin^4\tfrac{1}{2}\theta\,, \tag{2.13}$$

and

$$\epsilon\equiv\frac{k^2/2k^{*2}}{k^2/2k^{*2}+(W^2/m^2)\tan^2\frac{1}{2}\theta}\,. \tag{2.14}$$

Table I gives the functions $h_{1,3,4,6}{}^{J^\pi}(\theta_{kq})$ for the cases $J^\pi=\frac{1}{2}\pm$, $\frac{3}{2}\pm$, $\frac{5}{2}\pm$, and $\frac{7}{2}\pm$. These are just special cases with $J=J'$ and $\pi=\pi'$ for the h's used in Appendix B.

If only the final electron is detected and in the case of a sharp resonance, Eq. (2.12) reduces to the Bjorken-Walecka formula[20] for exciting a discrete nucleon resonance[21]

$$\frac{d\sigma_L}{d\Omega_2}=\frac{\sigma_M}{1+(2\epsilon_1/m)\sin^2\frac{1}{2}\theta}\left\{\frac{k^4}{k^{*4}}|f_c|^2+\left(\frac{k^2}{2k^{*2}}+\frac{W_R{}^2}{m^2}\tan^2\tfrac{1}{2}\theta\right)(|f_+|^2+|f_-|^2)\right\}, \tag{2.15}$$

provided that we identify

$$|f_+|^2=\frac{J+\frac{1}{2}}{k^*}\left[\int|T_{1/2,3/2}{}^{J^\pi}(W,k^2)_{\rm res}|^2dW\right],$$
$$|f_-|^2=\frac{J+\frac{1}{2}}{k^*}\left[\int|T_{1/2,1/2}{}^{J^\pi}(W,k^2)_{\rm res}|^2dW\right], \tag{2.16}$$
$$|f_c|^2=\frac{J+\frac{1}{2}}{k^*}\left[\int|T_{1/2,c}{}^{J^\pi}(W,k^2)_{\rm res}|^2dW\right].$$

The separation of the resonant parts of $T_{1/2,3/2}{}^{J^\pi}$, $T_{1/2,1/2}{}^{J^\pi}$, and $T_{1/2,c}{}^{J^\pi}$ and their connection with the amplitudes f_+, f_-, and f_c are discussed in Appendix A.

Some general features of the coincidence cross section should be noted. The dependence on the angle ϕ_{kq} is of particular interest because it is associated with the interference between helicity amplitudes. The $(\mathcal{J}^{+1})^*(\mathcal{J}^{-1})$ term leads to a $\cos2\phi_{kq}$ dependence, while the $\mathcal{J}_c{}^*(\mathcal{J}^{+1}+\mathcal{J}^{-1})$ term produces a $\sin\phi_{kq}$ dependence. The partial-wave expansion in terms of helicity matrix elements [Eq. (2.12) and Appendix B] is much simpler than is the expansion in terms of the conventional multipole amplitudes $E_{l\pm}$, $M_{l\pm}$, and $C_{l\pm}$.[10] For example, the $T_{1/2,3/2}{}^{J^\pi}$ terms do not contribute at $\theta_{kq}=0$ or π, and for one partial wave there is no $T_{1/2,c}{}^{J^\pi*}T_{1/2,1/2}{}^{J^\pi}$ interference. The relation between the multipoles $E_{l\pm}$, $M_{l\pm}$, and $C_{l\pm}$ and the helicity matrix elements is given in Appendix A. Finally, we see from Table I that a resonance of given spin produces a characteristic angular dependence. Thus the spin of a resonance can be deduced from the measured angular dependence of the cross section. The highest power of $\cos\theta_{kq}$ that appears for a resonance of spin J is $2J-1$. Thus for a $J=\frac{1}{2}$ resonance, the resonance cross section will have no angular dependence.

At $\theta_{kq}=0$ and π, the coincidence cross section has a particularly simple form:

$$\frac{d^5\sigma_L(\theta_{kq}=0,\pi)}{d\epsilon_2d\Omega_2d\Omega_q{}^*/4\pi}=\frac{m}{W}\sigma_M\frac{k^2}{2k^{*2}\epsilon}\frac{1}{k^*}\times\sum_{J^\pi,J'^{\pi'}}[2\epsilon(k^2/k^{*2})h_1\,{\rm Re}T_{1/2,c}{}^{J^\pi*}T_{1/2,c}{}^{J'^{\pi'}}+h_2\,{\rm Re}T_{1/2,1/2}{}^{J^\pi*}T_{1/2,1/2}{}^{J'^{\pi'}}]_{\theta_{kq}=0,\pi}\,. \tag{2.17}$$

The functions h_1 and h_2 depend on J^π, $J'^{\pi'}$, and θ_{kq}, and are given in Appendix B. It is thus possible to separate the $T_{1/2,1/2}{}^{J^\pi*}T_{1/2,1/2}{}^{J'^{\pi'}}$ from the $T_{1/2,c}{}^{J^\pi*}T_{1/2,c}{}^{J'^{\pi'}}$ terms by making a Rosenbluth plot for the coincidence cross section at $\theta_{kq}=0$ or π. As Baba *et al.*[5] have emphasized, there are many advantages to this procedure over a Rosenbluth plot for the noncoincidence cross section. After all, the noncoincidence separation yields only the contribution $|T_{1/2,1/2}{}^{J^\pi}|^2+|T_{1/2,3/2}{}^{J^\pi}|^2$, and if the helicity $\frac{3}{2}$ term is large, it is much more difficult to separate a small Coulomb contribution by this method. In terms of resonant parts, the $\theta_{kq}=0$ or π data determine f_- and f_c, and then f_+ can be found from comparison with the total cross section.

There is a special reason for making an effort to determine the product $|T_{1/2,1/2}{}^{l\pm}||T_{1/2,c}{}^{l\pm}|$ through coincidence experiments. The noncoincidence cross section for scattering of electrons from a polarized target[22] contains the term

$$(\mathbf{P}\cdot\hat{e}_{k1})\sigma_M\frac{m}{W}\left(\frac{k^2}{2k^{*2}\epsilon}\right)\frac{2}{k^*}\left[\frac{k^2}{k^{*2}}\epsilon(\epsilon+1)\right]^{1/2}\times\sum_{J^\pi}(J+\tfrac{1}{2})\,{\rm Im}(\pm T_{1/2,c}{}^{l\pm*}T_{1/2,1/2}{}^{l\pm})\,, \tag{2.18}$$

[20] J. D. Bjorken and J. D. Walecka, Ann. Phys. (N. Y.) **38**, 35 (1966).

[21] The density-of-states factor $[1+2(\epsilon_1/m)\sin^2(\frac{1}{2}\theta)]^{-1}$ is valid only if ϵ_1 and θ are kept fixed. If instead k^2 and θ are held fixed, then a different factor is present. This problem is discussed in Appendix A, where the relevant expressions are given.

[22] The *coincidence* cross section for electroproduction of pions from a polarized target has been discussed by N. Zagury and A. F. F. Teixeira, Nuovo Cimento **61A**, 83 (1969).

where $\mathbf{P}$ is the polarization of the target. If $\mathrm{Im}T_{1/2,1/2}{}^{l\pm}T_{1/2,c}{}^{l\pm *}\neq 0$, this term will lead to an asymmetry in the scattering depending upon whether the target polarization is up or down. Christ and Lee[13] have proposed looking for such an asymmetry in order to test time-reversal (T) invariance in the electromagnetic interactions of hadrons. They reason that a violation of T invariance would result in a phase difference δ between $T_{1/2,1/2}{}^{l\pm}$ and $T_{1/2,c}{}^{l\pm}$. The resulting asymmetry would thus be proportional to $|T_{1/2,1/2}{}^{l\pm}||T_{1/2,c}{}^{l\pm}|\sin\delta$. In order to conclude anything about δ from a search for such an asymmetry, one needs to know the value of $|T_{1/2,1/2}{}^{l\pm}||T_{1/2,c}{}^{l\pm}|$. Since this quantity can be determined from coincidence experiments at $\theta_{kq}=0$ or π, it would be useful to perform such experiments over as large a range of k^2 and W as possible. Experiments performed so far have detected no asymmetry,[23] but a knowledge of $|T_{1/2,1/2}{}^{l\pm}||T_{1/2,c}{}^{l\pm}|$ may suggest looking in different regions of the inelastic spectrum than have been investigated so far.

III. COUPLED-CHANNEL N/D MODEL

In this section we present predictions of a covariant, gauge-invariant model for the inelastic form factors f_+, f_-, and f_c. The predictions of the model agree well with the noncoincidence data, but comparison of the individual f's (presented here for the first time) with results of coincidence experiments will constitute a much more stringent test of the model.

Detailed explanations of this model have been presented previously,[7,8] and so only a brief review will be given here. Let $a(W,k^2)$ denote a particular electroproduction amplitude for producing a state of definite spin, parity, and isospin. As indicated schematically in Fig. 3, $a(W,k^2)$ is considered to be the result of two separate processes. First the nucleon is excited by the virtual photon to produce an intermediate state such as $|\pi N\rangle$ or $|\pi N^*\rangle$. The excitation of this state is described by a set of exchange graphs. The appropriate helicity projections of these graphs, denoted by $a^{\mathrm{lhs}}(W,k^2)$, give the contribution to the amplitude under consideration. The strong interactions, which depend only on the total c.m. energy W, then act in this state to build up a phase and create a resonance at the appropriate mass.

The simplest calculation one can perform within this framework is to keep only the $|\pi N\rangle$ intermediate state.[8] The expression for a resonant amplitude then takes the form

$$a(W,k^2)=a^{\mathrm{lhs}}(W,k^2)/D(W)\,, \tag{3.1}$$

where $D(W)$ is a final-state interaction factor. The amplitude thus has built into it the correct threshold and analyticity properties. In addition, in the elastic region it satisfies the final-state theorem and is an approximate solution of the Omnès equation.

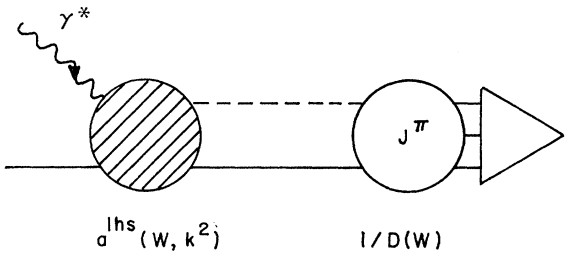

FIG. 3. Model for electroproduction of nucleon resonances.

For resonances other than $N^*(1236)$ a realistic calculation must include the effect of inelastic intermediate states. A more sophisticated calculation has been performed[7] in which the $|\pi N^*(1236)\rangle$ state is kept in addition to the $|\pi N\rangle$ state.[24] It is then assumed that only one linear combination, or one eigenchannel, of these two strong-interaction channels is resonant. The other eigenphase shift is assumed to be small. The production amplitude in this resonant eigenchannel is given by

$$A(W,k^2)=[a_1{}^{\mathrm{lhs}}(W,k^2)\cos\zeta+a_2{}^{\mathrm{lhs}}(W,k^2)\sin\zeta]/D(W)\,. \tag{3.2}$$

The mixing angle ζ is related to the partial widths for decay into channels 1 and 2 by

$$\cos^2\zeta=\Gamma_1/\Gamma\,, \tag{3.3}$$

$$\sin^2\zeta=\Gamma_2/\Gamma\,. \tag{3.4}$$

The amplitude for production of the resonance followed by decay into channel 1 is obtained by multiplying Eq. (3.2) by $\cos\zeta$. $D(W)$ is related to the *real* eigenphase shift ξ by

$$D(W)=\exp\left(-\frac{(W-M_s)}{\pi}\times\int_{W_0}^{\infty}\frac{\xi(W')dW'}{(W'-M_s)(W'-W-i\eta)}\right), \tag{3.5}$$

$$D(M_s)=1\,. \tag{3.6}$$

ξ can be obtained from the results of phase-shift analyses of πN scattering, and thus the shapes of the resonances are also obtained in this calculation. The subtraction is included since it appears that $\xi\to\frac{1}{2}\pi$ asymptotically. The unknown M_s is found[7] by normalizing to the data and, interestingly enough, turns out to be approximately equal to the nucleon mass for all resonances considered. This two-channel calculation has been performed for the states $\frac{3}{2}^+,\frac{3}{2}(1236)$[25]; $\frac{3}{2}^-,\frac{1}{2}(1525)$; $\frac{5}{2}^-,\frac{1}{2}(1680)$; $\frac{5}{2}^+,\frac{1}{2}(1688)$; and $\frac{7}{2}^+,\frac{3}{2}(1950)$. The $J^\pi=\frac{1}{2}^-$, $I=\frac{1}{2}$ partial wave contains two overlapping resonances, one of which

[23] J. R. Chen, J. Sanderson, J. A. Appel, G. Gladding, M. Goitein, K. Hanson, D. C. Imrie, T. Kirk, R. Madaras, R. V. Pound, L. Price, Richard Wilson, and C. Zajde, Phys. Rev. Letters **21**, 1279 (1968).

[24] Only the $|\pi N^*(1236)\rangle$ channel corresponding to the lower orbital angular momentum is included.

[25] For this resonance the mixing angle $\zeta\equiv 0$.

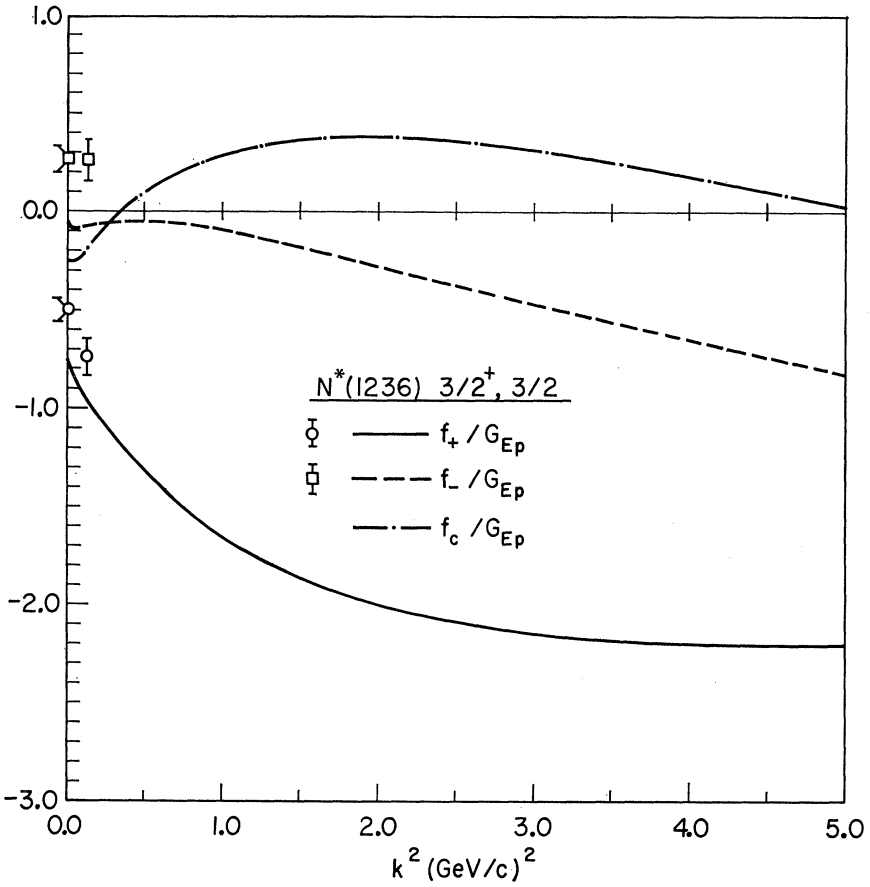

FIG. 4. f_+/G_{Ep}, f_-/G_{Ep}, and f_c/G_{Ep} for the $\frac{3}{2}^+,\frac{3}{2}(1236)$ resonance. The resonant part of the coincidence cross section can be found using Eqs. (A22)–(A25), (A31), and (2.12). The points at $k^2=0$ are obtained from the photoproduction analysis of Ref. 27. The magnitudes of the points at $k^2=3$ fm^{-2} are from Refs. 5 ($|f_-|^2$) and 26 ($|f_+|^2+|f_-|^2$); the signs are taken to be the same as those at $k^2=0$.

decays largely into $|N\eta\rangle$. For this partial wave it is no longer sufficient to assume that only one eigenchannel is resonant and to approximate all inelastic effects by the $|\pi N^*(1236)\rangle$ channel.

As excitation mechanisms for the $|\pi N\rangle$ and $|\pi N^*(1236)\rangle$ states, π, ω, N, and the convection current part of $N^*(1236)$ exchange are used. All the necessary coupling constants are known except for the *sign* of the combination $g_{\omega\pi\gamma}g_{\omega NN}$, and this sign is crucial. With the present choice of sign, it is the high-spin resonances which dominate the inelastic spectrum, and the $J=\frac{1}{2}$ contributions are unimportant. In the simple one-channel calculation, the opposite sign of this quantity gives a qualitatively different fit to the resonance cross section in the second and third resonance regions with the $J=\frac{1}{2}$ states dominating the spectrum for $k^2>0$. The fact that the two-channel calculation, which makes an attempt to include inelastic effects, produces qualitatively reasonable spectra in W at all k^2 is the strongest theoretical reason for believing that the high-spin states do in fact dominate the resonance spectrum. *The actual determination of the resonance spins in electron scattering, particularly as regards the role of the $J=\frac{1}{2}$ resonances, will be one of the most useful results to be obtained from coincidence experiments.*

Figure 4 presents the predictions for the individual amplitudes f_+, f_-, and f_c for the $\frac{3}{2}^+,\frac{3}{2}(1236)$ resonance. Decays into states other than $|\pi N\rangle$ are negligible for this resonance. Figures 5–9 give the predictions for exciting higher resonances followed by decay into the $|\pi N\rangle$ channel. These are the results of interest for coincidence experiments that detect only the $|\pi N\rangle$ final state. The two-channel predictions for the $\frac{3}{2}^-,\frac{1}{2}(1525)$ resonance are shown in Fig. 5, while for comparison, and to attempt to get some feel for the model dependence of these results, the one-channel predictions for this same state are given in Fig. 6. We emphasize again that the two-channel calculation is the more realistic one. Figures 7–9 give the two-channel predictions for the $\frac{5}{2}^+,\frac{1}{2}(1688)$; $\frac{5}{2}^-,\frac{1}{2}(1680)$; and $\frac{7}{2}^+,\frac{3}{2}(1950)$ resonances, respectively. The one-channel predictions for these resonances are fairly similar.

To obtain the correct helicity amplitudes for all k^2 is a severe test of any theory and clearly involves the detailed dynamics of the strong interactions. The predictions of the present model can probably be expected to give only a qualitative indication of the true behavior. In particular, comparison with the photoproduction results shown in Figs. 4, 5, and 7 gives some idea of the reliability of the predictions. However, comparison with the noncoincidence data shows that the model appears to provide a much better description away from $k^2=0$.[7,8]

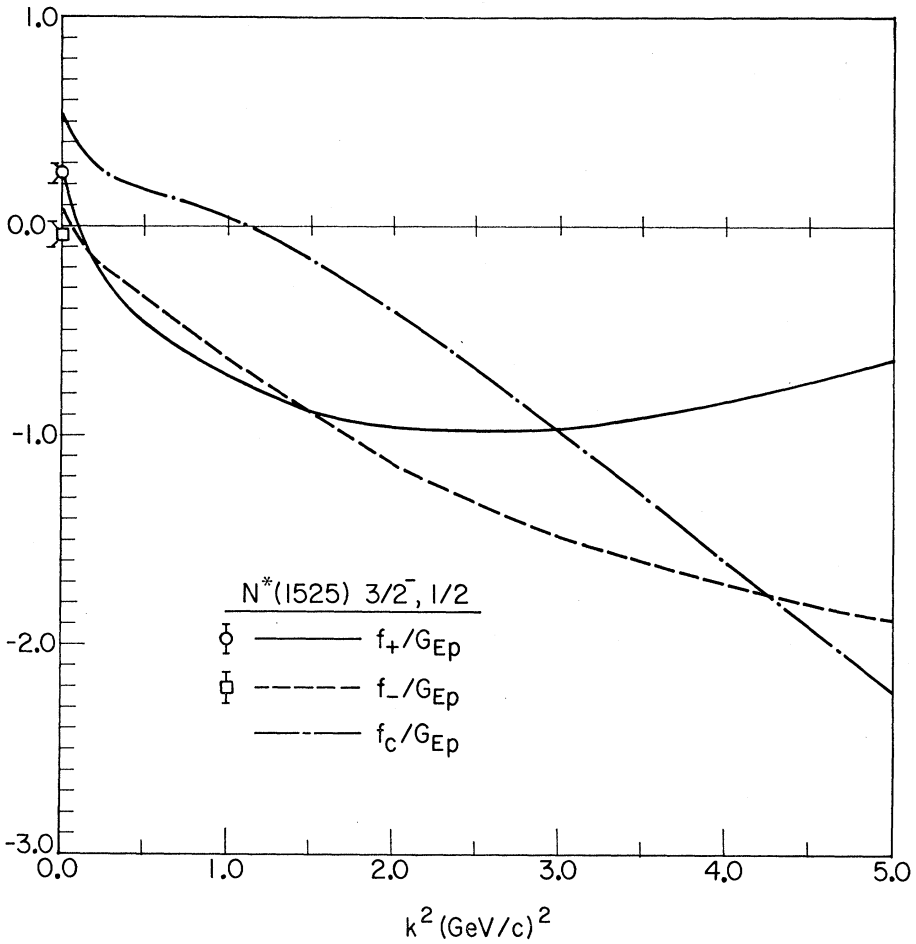

FIG. 5. Predictions of two-channel calculation for f_+/G_{Ep}, f_-/G_{Ep}, and f_c/G_{Ep} for excitation of the $\frac{3}{2}^-,\frac{1}{2}(1525)$ resonance followed by decay into the $|\pi N\rangle$ final state. The points at $k^2=0$ are obtained from the photoproduction analysis of Ref. 27.

IV. IMPLICATIONS FOR COINCIDENCE EXPERIMENTS

We now use the results of the previous section to discuss specific features of the resonances that should be observable in coincidence experiments.

(*i*) $\frac{3}{2}^+,\frac{3}{2}(1236)$. One of the more striking predictions for this resonance is the existence of a diffraction minimum in $|f_c|^2$ near $k^2=0.4$ GeV^2. The total cross-section measurements of Lynch *et al.*[26] appear to show such a minimum, but one cannot tell whether this is a property of the resonance or of the background. The π^0 coincidence experiment of Mistretta *et al.*[3] offers additional support. They detected a Coulomb-transverse interference at $k^2=0.13$ and 0.24 GeV^2 but found none at 0.4 GeV^2. Future coincidence experiments should attempt to confirm the presence of this zero in the resonant amplitude. In particular one would expect to see a Coulomb-transverse interference for $k^2>0.4$ GeV^2.

A second prediction is that $|f_+|^2$ completely dominates the transverse contribution. In photoproduction this is not the case since $f_+/f_-=-2.10\pm0.50$.[27] The experiment of Baba *et al.*,[5] however, indicates that $|f_-|^2$ decreases considerably between $k^2=0$ and $k^2=3$ fm^{-2} (0.12 GeV^2). Combining this measurement with the results of Lynch *et al.*[26] (which showed that $|f_+|^2+|f_-|^2$ increases slightly over this range), we estimate that $|f_+|/|f_-|=3.02\pm1.43$ at $k^2=3$ fm^{-2}. Thus it is possible that $|f_+|\gg|f_-|$ away from $k^2=0$.

(*ii*) *Second resonance.* There are two resonances in this region: $\frac{3}{2}^-,\frac{1}{2}(1525)$ and $\frac{1}{2}^-,\frac{1}{2}(1550)$. At $k^2=0$ this resonance region is known to be dominated by the $\frac{3}{2}^-$ state.[27] While there is *theoretical* evidence that the $\frac{3}{2}^-$ state dominates at all k^2 as discussed previously, it is crucial to have an experimental determination of the spin of this resonance for $k^2\neq0$. From Table I we see that the cross section for a pure spin-$\frac{1}{2}$ state has no θ_{kq} or ϕ_{kq} dependence. It should thus be possible to obtain a clear-cut experimental decision between spin $\frac{1}{2}$ and $\frac{3}{2}$.[28]

The results of the two-channel calculation for the $\frac{3}{2}^-$ state contain some interesting features. All three amplitudes f_+, f_-, and f_c are predicted to have zeros. It is

[26] H. L. Lynch, J. V. Allaby, and D. M. Ritson, Phys. Rev. **164**, 1635 (1967).

[27] R. L. Walker, Phys. Rev. **182**, 1729 (1969); S. D. Ecklund and R. L. Walker, *ibid.* **159**, 1195 (1967).

[28] If the $\frac{1}{2}^-$ state becomes dominant, the angular dependence should disappear at large k^2, but in the transition region angular dependence can arise from interference between the $\frac{3}{2}^-$ and $\frac{1}{2}^-$ states. In such a case one would expect a large $\cos2\phi_{kq}\sin^2\theta_{kq}$ term resulting from the interference of $T_{1/2,3/2}{}^{3/2-}$ and $T_{1/2,1/2}{}^{1/2-}$.

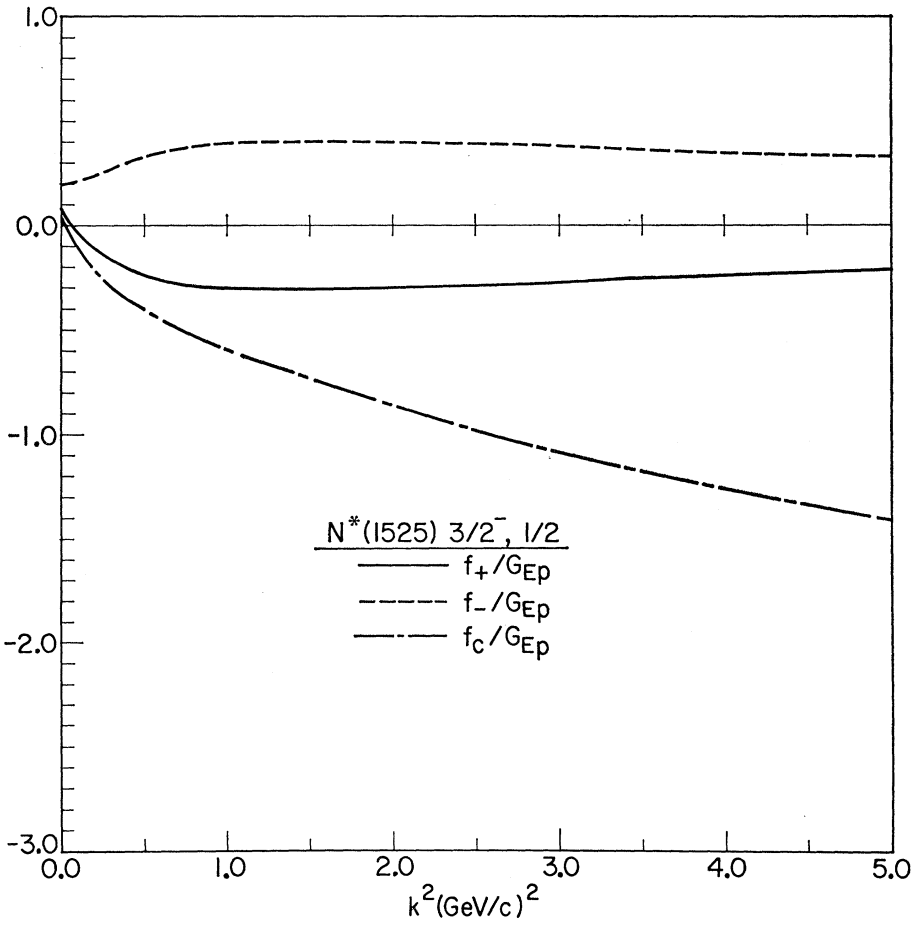

FIG. 6. Same as Fig. 5 except now predictions of one-channel calculation are given.

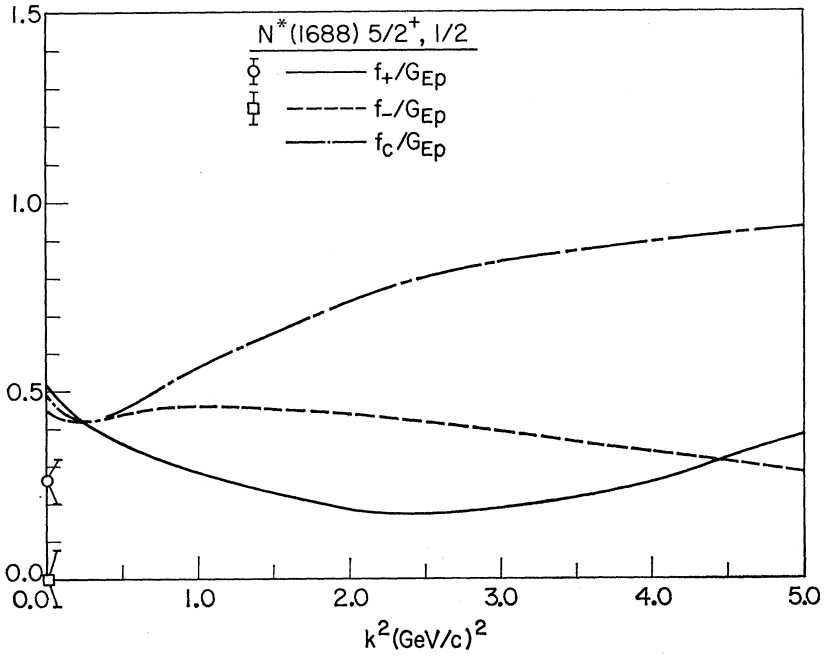

FIG. 7. Same as Fig. 5 for the $\frac{5}{2}^+,\frac{1}{2}(1688)$ resonance.

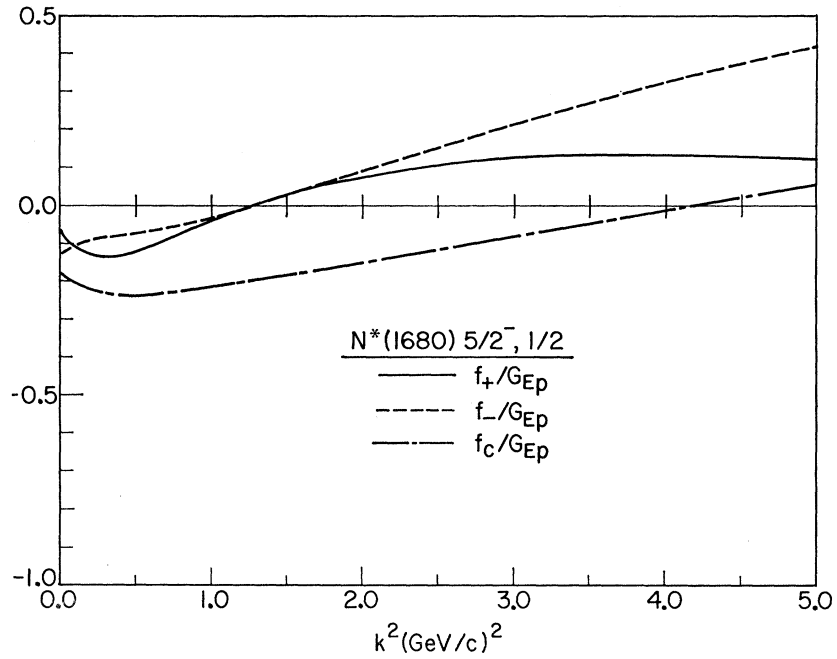

FIG. 8. Same as Fig. 5 for the $\frac{5}{2}^-,\frac{1}{2}(1680)$ resonance.

interesting to observe how the relative importance of the three amplitudes changes with k^2. In particular, the ratio f_+/f_- varies quite rapidly for small changes in k^2 above zero.

We thus see that a complete separation of the form factors for the second resonance in the low k^2 region ($0<k^2\lesssim 0.5$ GeV^2) would be extremely useful.

(iii) Third resonance. There are four well-established

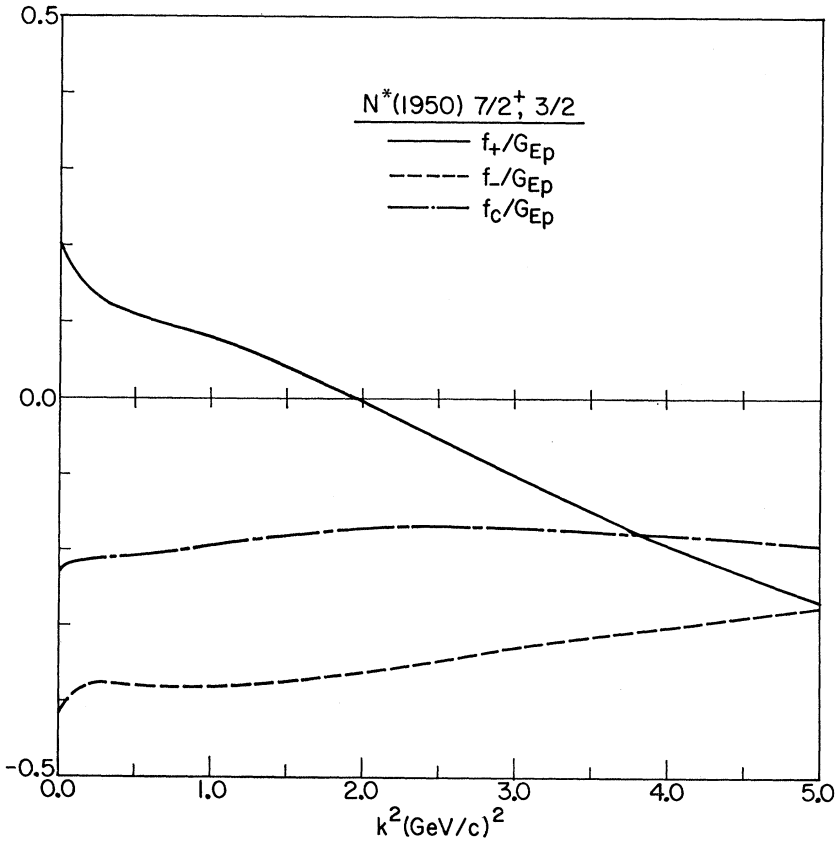

FIG. 9. Same as Fig. 5 for the $\frac{7}{2}^+,\frac{3}{2}(1950)$ resonance.

resonances in this region: $\frac{5}{2}^+,\frac{1}{2}(1688)$; $\frac{5}{2}^-,\frac{1}{2}(1680)$; $\frac{1}{2}^-,\frac{1}{2}(1710)$; and $\frac{1}{2}^-,\frac{3}{2}(1640)$. In photoproduction the two spin-$\frac{5}{2}$ states are dominant.[27] But just as in the second resonance region, it is crucial to have an experimental determination of the resonance spin in this region for $k^2\neq 0$.

Both the one-channel and two-channel calculations for the spin-$\frac{5}{2}$ states do not give good fits to the low-k^2 data.[7,8] If experiments show that the spin-$\frac{5}{2}$ states do indeed remain dominant in this region, the results of these experiments will be useful as a guide in attempting to improve the calculation for these states. Using the same subtraction point in the final-state enhancement factors for these two states, however, the two-channel calculation was able to obtain the experimental value 0.07 ± 0.03[27] for the ratio of the $\frac{5}{2}^-$ to the $\frac{5}{2}^+$ state in photoproduction. From Figs. 7 and 8 we see that for $k^2\neq 0$ the $\frac{5}{2}^-$ amplitudes are predicted to remain small relative to the dominant $\frac{5}{2}^+$ amplitudes, and one would like to confirm this in the coincidence experiments. Relative sizes of amplitudes for these two states can be determined from the $\frac{5}{2}^+$-$\frac{5}{2}^-$ interference, which contains terms with one higher power of $\cos\theta_{kq}$ than do the corresponding terms for a pure $\frac{5}{2}^+$ or $\frac{5}{2}^-$ state. To decide whether a particular amplitude belongs to the $\frac{5}{2}^+$ or $\frac{5}{2}^-$ state is not easy. It may be possible to determine the parity by looking for an interference between the second and third resonances.[27] For example, if the second resonance is taken to be $\frac{3}{2}^-$, then only odd powers of $\cos\theta_{kq}$ enter if the interference is with the $\frac{5}{2}^+$ amplitude, while only even powers enter if it is with the $\frac{5}{2}^-$.[29]

(iv) Fourth resonance. In pion-nucleon scattering this resonance is the $\frac{7}{2}^+,\frac{3}{2}(1950)$ state, and photoproduction experiments indicate a spin-$\frac{7}{2}$ resonance in this energy region.[27] In the total cross-section experiments it has been very difficult to see this resonance because of the large background, and consequently very little has been learned about the excitation of this state. In coincidence experiments this state can be identified by looking for a $\cos^6\theta_{kq}$ dependence in the cross section. Any information that is obtained concerning the excitation of this resonance will be useful.

V. SUMMARY

We have attempted to indicate the important role that coincidence experiments can play in obtaining an understanding of the nucleon resonances, and we have discussed some procedures that simplify the determination of the inelastic form factors. In order to obtain some specific predictions, we have presented and discussed the detailed results of a coupled-channel relativistic N/D model for nucleon levels in the first four resonance regions. These results have emphasized several important questions concerning the structure of the nucleon that can be answered by coincidence experiments. First of all, what is the role of the $J=\frac{1}{2}$ resonances? An experimental determination of the resonance spin for $k^2>0$ will decide if the $J=\frac{1}{2}$ resonances do grow in importance away from photoproduction. Do the individual form factors possess detailed structure such as zeros even though the total cross section appears to be a smooth function of k^2? Also, does one particular form factor tend to dominate the others at large k^2?

It is hoped that the discussion given here will prove useful in planning coincidence experiments. In addition, comparison of the results of such experiments with the predictions discussed above will permit a much more stringent test of the present model and contribute to a better understanding of the nucleon resonances.

[29] This is true for all terms except the Coulomb-transverse. Here the form of the interference with the $\frac{5}{2}^+$ amplitude is $\sin\theta_{kq}(\cos\theta_{kq})^{2n}$ and with the $\frac{5}{2}^-$ amplitude is $\sin\theta_{kq}(\cos\theta_{kq})^{2n+1}$, n an integer.

ACKNOWLEDGMENT

The authors are grateful to Professor J. D. Walecka for his useful criticisms and many helpful discussions.

APPENDIX A

A problem we have encountered in discussions with both experimentalists and theorists is the wide variety of notations, formulations, and phase conventions used in analyzing electroproduction. In this Appendix we discuss and relate various commonly used notations and formulations while explicitly explaining the conventions and formulations we have used. We shall also examine some of the special considerations that enter when a fit of the resonance shape is performed or an integration over final energy is carried out.

For simplicity and convenience we have chosen to work with helicity matrix elements rather than the more traditional multipole moments. The many phase conventions contained in our definition of the helicity matrix elements (see Sec. II) are most easily summarized by giving the relation to the traditional multipoles used by Chew, Goldberger, Low, and Nambu,[30] Zagury,[31] and others:

$$(4k^*q)^{1/2}(l+1)M_{l+} = -i\tfrac{1}{2}\sqrt{2}\{T_{1/2,1/2}{}^{l+}-[(l+2)/l]^{1/2}T_{1/2,3/2}{}^{l+}\}, \quad \text{(A1)}$$

$$(4k^*q)^{1/2}(l+1)E_{l+} = -i\tfrac{1}{2}\sqrt{2}\{T_{1/2,1/2}{}^{l+}+[l/(l+2)]^{1/2}T_{1/2,3/2}{}^{l+}\}, \quad \text{(A2)}$$

$$(4k^*q)^{1/2}lM_{l-} = -i\tfrac{1}{2}\sqrt{2}\{T_{1/2,1/2}{}^{l-} -[(l-1)/(l+1)]^{1/2}T_{1/2,3/2}{}^{l-}\}, \quad \text{(A3)}$$

$$(4k^*q)^{1/2}lE_{l-} = i\tfrac{1}{2}\sqrt{2}\{T_{1/2,1/2}{}^{l-} +[(l+1)/(l-1)]^{1/2}T_{1/2,3/2}{}^{l-}\}, \quad \text{(A4)}$$

$$(4k^*q)^{1/2}C_{l\pm}=iT_{1/2,c}{}^{l\pm}. \quad \text{(A5)}$$

[30] G. F. Chew, M. L. Goldberger, F. E. Low, and Y. Nambu, Phys. Rev. **106**, 1345 (1957).

[31] N. Zagury, Phys. Rev. **145**, 1112 (1966); **150**, 1406(E) (1966); **165**, 1934(E) (1968).

Depending on how the kinematic factors are treated, there are several ways of writing the inelastic cross section. We illustrate with the simple noncoincidence formula, and then in Appendix B choose a convenient notation and give the general unpolarized coincidence formula.

The approach of Drell and Walecka[32] uses the Mott cross section to isolate the electron kinematics. (Here, as everywhere else in this paper, we assume the electron mass is negligible.)

$$\frac{d^2\sigma_L}{d\Omega_2 d\epsilon_2}=\frac{1}{m}\sigma_M\sum_{J^\pi}\left[W_2{}^{J^\pi}(W,k^2)+2W_1{}^{J^\pi}(W,k^2)\tan^2\tfrac{1}{2}\theta\right], \quad \text{(A6)}$$

$$\sigma_M\equiv(\alpha^2\cos^2\tfrac{1}{2}\theta)/4\epsilon_1{}^2\sin^4\tfrac{1}{2}\theta. \quad \text{(A7)}$$

Here ϵ_1 and ϵ_2 refer to the electron laboratory energies and θ and Ω to the electron lab angles. It is convenient, however, to display the transverse and Coulomb excitations separately in terms of the helicity matrix elements. From the definition of W_1 and W_2 in terms of the matrix elements of the current operator, we find[33]

$$W_1{}^{J^\pi}=\tfrac{1}{2}W[(J+\tfrac{1}{2})/k^*]\times(|T_{1/2,1/2}{}^{J^\pi}|^2+|T_{1/2,3/2}{}^{J^\pi}|^2), \quad \text{(A8)}$$

$$W_2{}^{J^\pi}=(m^2/W)[(J+\tfrac{1}{2})/k^*]\{(k^4/k^{*4})|T_{1/2,c}{}^{J^\pi}|^2+(k^2/2k^{*2})[|T_{1/2,1/2}{}^{J^\pi}|^2+|T_{1/2,3/2}{}^{J^\pi}|^2]\}, \quad \text{(A9)}$$

with the result

$$\frac{d^2\sigma_L}{d\Omega_2 d\epsilon_2}=\frac{m}{W}\sigma_M\sum_{J^\pi}\left(\frac{J+\frac{1}{2}}{k^*}\right)\left[\frac{k^4}{k^{*4}}|T_{1/2,c}{}^{J^\pi}|^2+\left(\frac{k^2}{2k^{*2}}+\frac{W^2}{m^2}\tan^2\tfrac{1}{2}\theta\right)\times(|T_{1/2,1/2}{}^{J^\pi}|^2+|T_{1/2,3/2}{}^{J^\pi}|^2)\right]. \quad \text{(A10)}$$

The c.m. momentum k^* is given in terms of W and k^2 by

$$k^{*2}=k^2+(k_0{}^{\text{c.m.}})^2=k^2+[(W^2-m^2-k^2)/2W]^2. \quad \text{(A11)}$$

Alternatively, Hand[34] discusses the inelastic cross section by isolating the kinematic factors that correspond to photoproduction. He introduces the extremely convenient parameter ϵ, whose definition is equivalent to the one in Eq. (2.14) or to

$$k^2/2k^{*2}\epsilon=[k^2/2k^{*2}+(W^2/m^2)\tan^2\tfrac{1}{2}\theta]. \quad \text{(A12)}$$

The cross section is then written

$$d^2\sigma_L/d\Omega_2 d\epsilon_2=\Gamma_t(\sigma_t+\epsilon\sigma_s), \quad \text{(A13)}$$

$$\Gamma_t=(k^2/2k^{*2}\epsilon)\sigma_M(m^2/W^2)(K/2\pi^2\alpha), \quad \text{(A14)}$$

$$K\equiv(W^2-m^2)/2m. \quad \text{(A15)}$$

The constant K can be interpreted as the lab energy of a real photon needed to give a c.m. total energy W. By comparison with (A10) we see that

$$\sigma_t=(W/m)(2\pi^2\alpha/K)\sum_{J^\pi}[(J+\tfrac{1}{2})/k^*]\times(|T_{1/2,1/2}{}^{J^\pi}|^2+|T_{1/2,3/2}{}^{J^\pi}|^2), \quad \text{(A16)}$$

$$\sigma_s=(W/m)(2\pi^2\alpha/K)\sum_{J^\pi}[(J+\tfrac{1}{2})/k^*]\times(2k^2/k^{*2})|T_{1/2,c}{}^{J^\pi}|^2. \quad \text{(A17)}$$

Although this procedure is convenient when the $k^2\to 0$ limit is taken, we prefer to avoid the introduction of such extra factors as $2\pi^2\alpha/K$ and therefore isolate the electron kinematics and use Eq. (A10). A very compact notation is to use the "virtual photon polarization" ϵ in Eq. (A10), giving

$$\frac{d^2\sigma_L}{d\Omega_2 d\epsilon_2}=\frac{m}{W}\sigma_M\frac{k^2}{2k^{*2}\epsilon}\sum_{J^\pi}\left(\frac{J+\frac{1}{2}}{k^*}\right)\left[2\epsilon\frac{k^2}{k^{*2}}|T_{1/2,c}{}^{J^\pi}|^2+|T_{1/2,1/2}{}^{J^\pi}|^2+|T_{1/2,3/2}{}^{J^\pi}|^2\right]. \quad \text{(A18)}$$

Note that as $\theta\to\pi$

$$\frac{k^2}{2k^{*2}\epsilon}\sigma_M\xrightarrow[\theta\to\pi]{}\frac{W^2}{m^2}\frac{\alpha^2}{4\epsilon_1{}^2}. \quad \text{(A19)}$$

The coincidence cross section in Appendix B uses the notation of (A18).

In the case of a resonance, it is desirable to isolate and integrate out the resonant W variation and thereby obtain inelastic form factors that depend only on k^2. We use form factors f_+, f_-, and f_c like those defined by Bjorken and Walecka[20] for the case of a stable isobar, and extend the definition to resonances of finite width. It is convenient to introduce a shape function $R(W)$ satisfying

$$\int|R(W)|^2dW=1, \quad \text{(A20)}$$

$$R(W_R)=|R(W_R)|e^{i\pi/2}, \quad \text{(A21)}$$

and then define resonant and background parts by writing

$$T^{J^\pi}(W,k^2)=T^{J^\pi}(k^2)_R R(W)+T^{J^\pi}(W,k^2)_B. \quad \text{(A22)}$$

This procedure is model-dependent in that just what value of the quantity $T^{J^\pi}(k^2)_R$ is extracted from fits to experimental data will depend on the specific shape assumed for $R(W)$. It is possible that one may eventually need to choose different functions R for different helicities or values of k^2, but until the data can distinguish such possibilities, a simple model for $R(W)$ is

[32] S. D. Drell and J. D. Walecka, Ann. Phys. (N. Y.) **28**, 18 (1964).

[33] For simplicity only the contribution of the $|\pi N\rangle$ final state is given. Contributions of other final states can be included in a similar fashion using the helicity formalism.

[34] L. N. Hand, Phys. Rev. **129**, 1834 (1963).

sufficient. Making the identification that $|R(W)|^2$ is a generalization of $\delta(W-W_R)$, we define for a given J^π

$$f_+(k^2)=-i[(J+\tfrac{1}{2})/k^*]^{1/2}T_{1/2,3/2}{}^{J^\pi}(k^2)_R, \quad \text{(A23)}$$

$$f_-(k^2)=-i[(J+\tfrac{1}{2})/k^*]^{1/2}T_{1/2,1/2}{}^{J^\pi}(k^2)_R, \quad \text{(A24)}$$

$$f_c(k^2)=+i[(J+\tfrac{1}{2})/k^*]^{1/2}T_{1/2,c}{}^{J^\pi}(k^2)_R, \quad \text{(A25)}$$

with k^* evaluated at $W=W_R$.[35]

In Figs. 4–9 we presented predictions for the form factors based on a model reviewed in Sec. III. We summarize here how that particular simple model defined $T^{J^\pi}(k^2)_R$ and $R(W)$. The resonant part of an helicity amplitude ($\lambda=\frac{1}{2}$, $\frac{3}{2}$, or c) leading to the $|\pi N\rangle$ channel is written

$$\cos\zeta(W)\,A_{1/2,\lambda}{}^{J^\pi}(W,k^2)^{\rm lhs}/D(W) = T_{1/2,\lambda}{}^{J^\pi}(k^2)_R R(W), \quad \text{(A26)}$$

where $D(W)$ is the eigenchannel denominator function satisfying the final-state theorem

$$D(W)=|D(W)|\exp[-i\xi(W)], \quad \text{(A27)}$$

with $\xi(W_R)=\frac{1}{2}\pi$. $A_{1/2,\lambda}{}^{J^\pi}(W,k^2)^{\rm lhs}$ is the excitation function described in Sec. III. The model assumes that in the vicinity of a resonance the numerator varies slowly and that the final-state enhancement factor can be expanded in a Taylor series:

$$D(W)\cong[{\rm Re}'D(W_R)][(W-W_R)+\tfrac{1}{2}i\Gamma]. \quad \text{(A28)}$$

The resonance is defined to be the place where

$${\rm Re}D(W)=0. \quad \text{(A29)}$$

Thus the model gives

$$\frac{\cos\zeta(W)\,A_{1/2,\lambda}{}^{J^\pi}(W,k^2)^{\rm lhs}}{D(W)} \cong \frac{\cos\zeta(W_R)\,A_{1/2,\lambda}{}^{J^\pi}(W_R,k^2)^{\rm lhs}}{{\rm Re}'D(W_R)} \times\frac{1}{W-W_R+\frac{1}{2}i\Gamma}, \quad \text{(A30)}$$

$$R(W)\cong-(\Gamma/2\pi)^{1/2}/[(W-W_R)+\tfrac{1}{2}i\Gamma], \quad \text{(A31)}$$

$$T_{1/2,\lambda}{}^{J^\pi}(k^2)_R \cong\frac{-(2\pi/\Gamma)^{1/2}\cos\zeta(W_R)\,A_{1/2,\lambda}{}^{J_\pi}(W_R,k^2)^{\rm lhs}}{{\rm Re}'D(W_R)}. \quad \text{(A32)}$$

We illustrate the integration over W with the noncoincidence cross section, and suppose for simplicity that we are dealing with a single resonance. The resonant part of the cross section is defined by

$$\left(\frac{d^2\sigma_L}{d\Omega_2 d\epsilon_2}\right)_R=\frac{m}{W}\sigma_M\frac{k^2}{2k^{*2}\epsilon}\left(\frac{J+\frac{1}{2}}{k^*}\right)[2\epsilon(k^2/k^{*2}) \times|T_{1/2,c}{}^{J^\pi}(k^2)_R|^2+|T_{1/2,1/2}{}^{J^\pi}(k^2)_R|^2 +|T_{1/2,3/2}{}^{J^\pi}(k^2)_R|^2]|R(W)|^2. \quad \text{(A33)}$$

In order to integrate over W, we need the Jacobian $\partial\epsilon_2/\partial W$, which has two values depending upon whether ϵ_1 or k^2 is held fixed throughout the integration. (We assume that θ is also fixed.)

$$\left(\frac{\partial\epsilon_2}{\partial W}\right)_{\theta,\epsilon_1}=-\frac{W}{m}\frac{\epsilon_2}{\epsilon_2+k^2/2m} =-\frac{W}{m}\frac{1}{1+2(\epsilon_1/m)\sin^2\frac{1}{2}\theta}, \quad \text{(A34)}$$

$$\left(\frac{\partial\epsilon_2}{\partial W}\right)_{\theta,k^2}=-\frac{W}{m}\frac{\epsilon_2}{\epsilon_2+\epsilon_1} =-\frac{W}{m}\frac{k^2}{k^2+4\epsilon_1{}^2\sin^2\frac{1}{2}\theta}. \quad \text{(A35)}$$

If k^2 is held fixed, and if the resonances are assumed to be sharp enough so that the kinematic factors ϵ_1, k^*, and ϵ [see Eq. (2.14)] may be evaluated on resonance, we obtain

$$\left(\frac{d\sigma_L}{d\Omega_2}\right)_R=\sigma_M\frac{k^2}{k^2+4\epsilon_1{}^2\sin^2\frac{1}{2}\theta}\frac{k^2}{2k^{*2}\epsilon} \times[2\epsilon(k^2/k^{*2})|f_c(k^2)|^2 +|f_+(k^2)|^2+|f_-(k^2)|^2], \quad \text{(A36)}$$

where everything is evaluated at $W=W_R$ and the f's have been introduced using (A23)–(A25). On the other hand, if ϵ_1 is held fixed, the assumption that all k^2 dependence in the kinematics and *in the form factors* can be evaluated at $W=W_R$ is needed to obtain the formula given in Eq. (2.15). Keeping k^2 fixed is evidently the more desirable procedure since any variation across the resonance then enters through *known* kinematic factors.

APPENDIX B

In this Appendix we give the coincidence cross section in terms of the helicity amplitudes and of the angles defined in Fig. 2. The general result follows from Eq. (2.6) after a Jacob-Wick expansion and a spin sum are

[35] In the limit of a sharp resonance, the f's defined above can be identified with those (denoted by $f^{\rm BW}$) used by Bjorken and Walecka (Ref. 20): $f_\pm{}^{\rm BW}=f_\pm$ and $f_c{}^{\rm BW}=-f_c$.

performed:

$$\frac{d^5\sigma_L}{d\epsilon_2 d\Omega_2 d\Omega_q{}^*/4\pi}=\frac{m}{W}\sigma_M\frac{k^2}{2k^{*2}\epsilon}\frac{1}{k^*}\sum_{J^\pi,J'^{\pi'}}\{2\epsilon(k^2/k^{*2})h_1\,\mathrm{Re}(T_{1/2,c}{}^{J^\pi *}T_{1/2,c}{}^{J'^{\pi'}})$$
$$+h_2\,\mathrm{Re}(T_{1/2,1/2}{}^{J^\pi *}T_{1/2,1/2}{}^{J'^{\pi'}})+h_3\,\mathrm{Re}(T_{1/2,3/2}{}^{J^\pi *}T_{1/2,3/2}{}^{J'^{\pi'}})$$
$$+2\epsilon\cos 2\phi_{kq}\,h_4\,\mathrm{Re}(T_{1/2,1/2}{}^{J^\pi *}T_{1/2,3/2}{}^{J'^{\pi}})+2[(k^2/k^{*2})\epsilon(\epsilon+1)]^{1/2}\sin\phi_{kq}\,h_5\,\mathrm{Re}(T_{1/2,c}{}^{J^\pi *}T_{1/2,1/2}{}^{J'^{\pi'}})$$
$$+2[(k^2/k^{*2})\epsilon(\epsilon+1)]^{1/2}\sin\phi_{kq}\,h_6\,\mathrm{Re}(T_{1/2,c}{}^{J^\pi *}T_{1/2,3/2}{}^{J'^{\pi'}})\}. \quad \text{(B1)}$$

The functions h_1–h_6 depend on J^π, $J'^{\pi'}$ and θ_{kq}, and are given below. The sum over J^π and $J'^{\pi'}$ is unconstrained.

For compactness we define a sign function by

$$S=+1 \quad \text{if} \quad \pi\pi'=(-1)^{J+J'+1}$$
$$=-1 \quad \text{if} \quad \pi\pi'=(-1)^{J+J'}. \quad \text{(B2)}$$

Equivalently, if the interfering states are both of normal or abnormal parity ($J=l+\frac{1}{2}$, $J'=l'+\frac{1}{2}$ or $J=l-\frac{1}{2}$, $J'=l'-\frac{1}{2}$) then $S=+1$, otherwise $S=-1$. Now we express the dependence on the c.m. angles in terms of derivatives of Legendre polynomials:

$$h_1=[\cos^2(\tfrac{1}{2}\theta_{kq})+S\sin^2(\tfrac{1}{2}\theta_{kq})](P_{J+1/2}{}'P_{J'+1/2}{}'+P_{J-1/2}{}'P_{J'-1/2}{}')$$
$$-[\cos^2(\tfrac{1}{2}\theta_{kq})-S\sin^2(\tfrac{1}{2}\theta_{kq})](P_{J+1/2}{}'P_{J'-1/2}{}'+P_{J-1/2}{}'P_{J'+1/2}{}'), \quad \text{(B3)}$$

$$h_2=[S\cos^2(\tfrac{1}{2}\theta_{kq})+\sin^2(\tfrac{1}{2}\theta_{kq})](P_{J+1/2}{}'P_{J'+1/2}{}'+P_{J-1/2}{}'P_{J'-1/2}{}')$$
$$-[S\cos^2(\tfrac{1}{2}\theta_{kq})-\sin^2(\tfrac{1}{2}\theta_{kq})](P_{J+1/2}{}'P_{J'-1/2}{}'+P_{J-1/2}{}'P_{J'+1/2}{}'), \quad \text{(B4)}$$

$$h_3=\{(\sin^2\theta_{kq})/[(J+\tfrac{3}{2})(J-\tfrac{1}{2})(J'+\tfrac{3}{2})(J'-\tfrac{1}{2})]^{1/2}\}$$
$$\times\{[\cos^2(\tfrac{1}{2}\theta_{kq})+S\sin^2(\tfrac{1}{2}\theta_{kq})](P_{J+1/2}{}''P_{J'+1/2}{}''+P_{J-1/2}{}''P_{J'-1/2}{}'')$$
$$-[\cos^2(\tfrac{1}{2}\theta_{kq})-S\sin^2(\tfrac{1}{2}\theta_{kq})](P_{J+1/2}{}''P_{J'-1/2}{}''+P_{J-1/2}{}''P_{J'+1/2}{}'')\}, \quad \text{(B5)}$$

$$\cos 2\phi_{kq}\,h_4=\cos 2\phi_{kq}\{\sin^2\theta_{kq}/[(J'+\tfrac{3}{2})(J'-\tfrac{1}{2})]^{1/2}\}$$
$$\times[\tfrac{1}{2}(S-1)(P_{J+1/2}{}'P_{J'+1/2}{}''-P_{J-1/2}{}'P_{J'-1/2}{}'')+\tfrac{1}{2}(S+1)(P_{J+1/2}{}'P_{J'-1/2}{}''-P_{J-1/2}{}'P_{J'+1/2}{}'')], \quad \text{(B6)}$$

$$\sin\phi_{kq}\,h_5=\sin\phi_{kq}\sin\theta_{kq}$$
$$\times[\tfrac{1}{2}(1-S)(P_{J+1/2}{}'P_{J'+1/2}{}'-P_{J-1/2}{}'P_{J'-1/2}{}')+\tfrac{1}{2}(1+S)(P_{J+1/2}{}'P_{J'-1/2}{}'-P_{J-1/2}{}'P_{J'+1/2}{}')], \quad \text{(B7)}$$

$$\sin\phi_{kq}\,h_6=\sin\phi_{kq}\{\sin\theta_{kq}/[(J'+\tfrac{3}{2})(J'-\tfrac{1}{2})]^{1/2}\}$$
$$\times\{[\cos^2(\tfrac{1}{2}\theta_{kq})+S\sin^2(\tfrac{1}{2}\theta_{kq})](P_{J+1/2}{}'P_{J'+1/2}{}''+P_{J-1/2}{}'P_{J'-1/2}{}'')$$
$$-[\cos^2(\tfrac{1}{2}\theta_{kq})-S\sin^2(\tfrac{1}{2}\theta_{kq})](P_{J+1/2}{}'P_{J'-1/2}{}''+P_{J-1/2}{}'P_{J'+1/2}{}'')\}. \quad \text{(B8)}$$

In the above, the primes indicate total derivatives of the Legendre polynomials. Thus,

$$P_{J+1/2}{}'\equiv\frac{d}{d(\cos\theta_{kq})}P_{J+1/2}(\cos\theta_{kq}). \quad \text{(B9)}$$

Note that if $J=J'$ and $\pi=\pi'$, then $h_1=h_2$ and $h_5=0$.